JOURNAL OF SPACECRAFT AND ROCKETS
Vol. 48, No. 1, January–February 2011

Prediction of Atomic Oxygen Erosion Yield for Spacecraft Polymers

Bruce A. Banks*
Alphaport, Inc., Cleveland, Ohio 44135
Jane A. Backus†
Ohio Aerospace Institute, Cleveland, Ohio 44142
Michael V. Manno†
Alphaport, Inc., Cleveland, Ohio 44135
Deborah L. Waters‡
ASRC Aerospace, Cleveland, Ohio 44135
Kevin C. Cameron†
Ohio Aerospace Institute, Brookpark, Ohio 44142
and
Kim K. de Groh§
NASA John H. Glenn Research Center at Lewis Field, Cleveland, Ohio 44135

DOI: 10.2514/1.48849

The ability to predict the atomic oxygen erosion yield of polymers based on their chemistry and physical properties has been only partially successful because of a lack of reliable low-Earth-orbit erosion yield data. The retrieval of the polymer erosion and contamination experiment after 3.95 years in low Earth orbit as part of the Materials International Space Station Experiment 2 provided accurate measurements of the erosion yields of 38 polymers and pyrolytic graphite. The resulting erosion yield data was used to develop a predictive tool with a correlation coefficient of 0.895 and uncertainty of $\pm 6.3 \times 10^{-25}$ cm^3/atom. The predictive tool uses the chemical structures and physical properties of polymers to predict in-space atomic oxygen erosion yields. A technique which uses the erosion yields of two materials is presented to allow prediction of the erosion yield of a composite material.

Nomenclature

A = mass fraction ash
$C_{C/t}$ = coefficient for the ratio of number of carbon atoms to total atoms in the repeat unit
$C_{Cl/C}$ = coefficient for the ratio of number of chlorine atoms to carbon atoms in the repeat unit
$C_{Cl/t}$ = coefficient for the ratio of number of chlorine atoms to total atoms in the repeat unit
$C_{dO/t}$ = coefficient for the ratio of number of double bonded oxygen atoms to total atoms in the repeat unit
$C_{F/C}$ = coefficient for the ratio of number of fluorine atoms to carbon atoms in the repeat unit
$C_{F/t}$ = coefficient for the ratio of number of fluorine atoms to total atoms in the repeat unit
$C_{H/C}$ = coefficient for the ratio of number of hydrogen atoms to carbon atoms in the repeat unit
$C_{H/t}$ = coefficient for the ratio of number of hydrogen atoms to total atoms in the repeat unit
$C_{N/C}$ = coefficient for the ratio of number of nitrogen atoms to carbon atoms in the repeat unit
$C_{N/t}$ = coefficient for the ratio of number of nitrogen atoms to total atoms in the repeat unit
$C_{O/C}$ = coefficient for the ratio of number of oxygen atoms to carbon atoms in the repeat unit
$C_{S/C}$ = coefficient for the ratio of number of sulfur atoms to carbon atoms in the repeat unit
$C_{sO/t}$ = coefficient for the ratio of number of single bonded oxygen atoms to total atoms in the repeat unit
$C_{S/t}$ = coefficient for the ratio of number of sulfur atoms to total atoms in the repeat unit
C_ρ = coefficient for the density of the material
$C_{\Sigma/r}$ = coefficient for ratio of the sum of the volume of the atoms making up the polymer repeat unit based on their covalent radii to actual volume of the repeat unit determined based on its chemical structure, molecular weight, and density
E_R = atomic oxygen erosion resistance, atoms/cm^3
E_{Rf} = atomic oxygen erosion resistance of fibers, atoms/cm^3
E_{Rp} = atomic oxygen erosion resistance of polymer matrix, atoms/cm^3
E_y = atomic oxygen erosion yield of a material, cm^3/atom
E_{yo} = Erosion yield of epoxy without any ash content in end hall test, atoms/cm^3
E_{ya} = erosion yield of epoxy with ash content, atoms/cm^3
E_{yf} = atomic oxygen erosion yield of the carbon fiber portion of the mixed material, cm^3/atom
E_{yp} = atomic oxygen erosion yield of the polymer portion of the mixed material, cm^3/atom
F = atomic oxygen fluence, atoms/cm^2
F_f = fractional volume fill of fibers in the composite
F_p = fractional volume fill of polymer in the composite
K = erosion yield attenuation constant
N_C = number of carbon atoms in the repeat unit

Received 7 January 2010; revision received 17 May 2010; accepted for publication 8 September 2010.

*Senior Physicist, Supporting NASA Space Experiments and Environments Branch, 21000 Brookpark Road, Mail Stop 309-2.
†Research Intern, Supporting NASA Space Experiments and Environments Branch, 21000 Brookpark Road, Mail Stop 309-2.
‡Research Chemist, Supporting NASA Space Experiments and Environments Branch, 21000 Brookpark Road, Mail Stop 309-2.
§Senior Materials Engineer, NASA Space Experiments and Environments Branch, 21000 Brookpark Road, Mail Stop 309-2.

N_{Cl} = number of chlorine atoms in the repeat unit
N_{dO} = number of double bonded oxygen atoms in the repeat unit
N_F = number of fluorine atoms in the repeat unit
N_H = number of hydrogen atoms in repeat unit
N_N = number of nitrogen atoms in the repeat unit
N_O = number of oxygen atoms in the repeat unit
N_S = number of sulfur atoms in the repeat unit
N_{sO} = number of single bonded oxygen atoms in the repeat unit
N_t = total number of atoms in the repeat unit
V_r = the actual volume of a repeat unit determined based on its chemical structure, molecular weight, and density, cm^3
V_Σ = sum of the volume of the atoms making up the polymer repeat unit based on their covalent radii, cm^3
ρ = density of the polymer, $grams/cm^3$

I. Introduction

EARLY space shuttle flight experiments found that hydrocarbon polymers exposed to the low-Earth-orbit (LEO) environment would gradually erode as a result of atomic oxygen exposure. The atomic oxygen interacts with the polymers causing the surface to convert to volatile oxidation products. The atomic oxygen erosion rates differed from one type of polymer to another [1–6]. This erosion susceptibility is measured as the atomic oxygen erosion yield, which is the volume lost per incident atomic oxygen atom, given in $cm^3/atom$ [7]. Numerous LEO flight experiments have been performed that have contributed to the available data on atomic oxygen erosion yields for a variety of materials. Many of the experiments were conducted on various short duration shuttle missions including STS-5 [1], STS-8 [8], and the evaluation of oxygen interactions with materials 3 experiment on STS-46 [9]. In addition, many materials were evaluated after lengthy LEO exposure (5.8 years) on the long duration exposure facility [10]. Unfortunately, many of these early experiments did not use dehydrated mass loss measurements, and the resulting mass loss due to atomic oxygen exposure may have been obscured because samples were often not in consistent states of dehydration during the preflight and postflight mass measurements. This is a particular problem for short duration mission exposures or low erosion yield materials. Inconsistent states of dehydration can cause erroneous erosion yields because polymer mass loss due to oxidation can be indistinguishable from changes in the amount of absorbed water in the polymer.

Forty different polymer samples, collectively called the polymer erosion and contamination experiment (PEACE) polymers, have been exposed to the LEO space environment on the exterior of the International Space Station (ISS) for nearly four years as part of Materials ISS Experiment 2 (MISSE 2). The purpose of the MISSE 2 PEACE polymers experiment was to accurately determine the atomic oxygen erosion yield of a wide variety of polymeric materials exposed for an extended period of time to the LEO space environment. The majority of samples were thin film polymers, flown with numerous layers stacked together [11,12]. Carefully obtained dehydrated preflight and postflight mass measurements, as well as accurate density measurements, were used to determine accurate high-fluence (8.43×10^{21} $atoms/cm^2$) erosion yield data for the MISSE 2 PEACE polymers samples [11,12]. For many samples, multiple layers of the polymers were used to insure that the materials would not be oxidized all the way through. The samples were also exposed to a total of 5000–6700 equivalent hours of solar radiation which included 650–820 h of Earth-reflected illumination [11].

The materials chosen for the MISSE 2 PEACE experiment were selected specifically to represent many polymers typically used in space as well as a wide variety of polymer chemical structures. The intent of choosing a variety of polymer structures was that the diversified data could assist with the development of an atomic oxygen erosion yield predictive tool. This tool could then be used to predict LEO erosion yields of new polymers based on chemical structure and simple low-cost ground laboratory test data, thus bypassing the need for actual in-space LEO testing for new polymers that are developed.

The dependence of atomic oxygen erosion yield on chemical structure has been explored based on early available LEO data [13–15]. A variety of approaches were considered in this paper to develop an erosion yield predictive formula based on best fit criteria to the MISSE 2 PEACE spaceflight data [12].

II. Erosion Yield Modeling Concepts

As a result of the atomic oxygen erosion yield investigation of polymers over several decades, it has become apparent that materials and polymers that form volatile oxidation products such as carbon and polymers have been found to have different atomic oxygen erosion yields. For example hydrocarbon polymers that have a high fraction of their atoms being oxygen such as polyoxymethylene tend to have higher erosion yields than those which have small fractional oxygen content. Polymers that have high fraction of fluorine atoms [such as fluorinated ethylene propylene (FEP) and polytetrafluoroethylene (PTFE) Teflon] tend to have lower atomic oxygen erosion yields that those having hydrogen instead of fluorine (such as polyethylene). Although the degree to which the type and number of chemical bonds of each type influence the probability of an atomic oxygen atom reacting is not clear, it is reasonable to assume that there is such a dependence on atomic oxygen erosion yield.

An oxidizable material with many atoms per cubic centimeter (such as carbon) should have a lower atomic oxygen erosion yield than one with few atoms per cubic centimeter (such as polystyrene foam) because it takes more oxygen atoms per square centimeter to oxidize a material with more atoms per cubic centimeter. Polymers that contain a high fraction of nonoxidizable content such as ash or metal oxide pigment particles (white Tedlar polyvinylfluoride) should have a lower erosion yield than polymers that have low ash content, because the nonoxidizable particles can shield the oxygen atoms from reacting with the polymer. Similarly as an ash-containing polymer erodes with time increasing portion of the polymer surface becomes covered with ash which should cause the erosion yield to drop with time or fluence. Thus, the atomic oxygen fluence was considered as a variable because almost all polymers contain a small amount of nonoxidizable ash.

The modeling information used to develop an atomic oxygen predictive tool consisted of the MISSE 2 PEACE polymers LEO atomic oxygen erosion yield data [11,12], polymer chemical structure information concerning the number and types of chemical bonds, polymer density information [11,12], fractional ash content data and atomic oxygen fluence. Although other environmental factors in addition to atomic oxygen such as vacuum ultraviolet radiation, ionizing radiation, and sample temperature may have effects on the erosion yield of materials, they were not included in this model because they were not varied in the MISSE 2 experiment. The atomic oxygen predictive tool equation coefficients were sequentially and iteratively adjusted to achieve the highest correlation coefficient between actual LEO results and those from using the predictive tool. Thus, for every physical property and chemical a degree discussed preceding, a dependence was assumed that was optimized to provide the closest match between predicted and actual erosion yields.

A. LEO Atomic Oxygen Erosion Yield Data from MISSE 2

Atomic oxygen erosion yield data was obtained from the MISSE 2 PEACE polymers experiment, which exposed 41 one-in. diam samples, including two Kapton H polyimide atomic oxygen fluence witness samples, to the LEO space environment. This experiment was flown in MISSE passive experiment container 2 tray 1, sample tray E5, which was attached to the exterior of the ISS Quest airlock, and placed in a ram facing orientation. This experiment was subjected to directed ram atomic oxygen along with solar and charged particle radiation and was exposed to the LEO environment for 3.95 years from 16 August 2001 to 30 July 2005. It was retrieved during a space walk on 30 July 2005 during Discovery's STS-114 return to flight mission. Figure 1 shows MISSE 2 on the ISS.

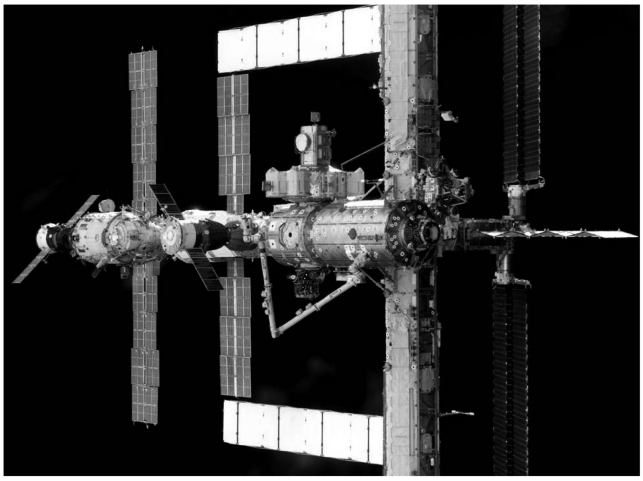

Fig. 1 MISSE 2 passive experiment carrier 2 tray 1 holding the PEACE polymers attached to the ISS 16 August 2001 to 30 July 2005.

Figures 2 and 3 show preflight and postflight photos of the MISSE 2 PEACE polymers experiment tray containing the 40 polymers and pyrolytic graphite.

Details of the specific polymers flown, flight sample fabrication, solar and ionizing radiation environmental exposure, preflight and postflight characterization techniques, and atomic oxygen fluence calculations are presented in [11,12]. The atomic oxygen fluence was found to be 8.43×10^{21} atoms/cm^2. Results of x-ray photoelectron spectroscopy contamination analysis of two MISSE 2 sapphire witness samples in tray E6 (located on the same MISSE surface and next to tray E5) indicated the space experiment had received very little contamination. An extremely thin silica contaminant layer of 1.3 and 1.4 nm was on each slide, respectively [10].

The MISSE 2 PEACE polymers experiment LEO atomic oxygen erosion yield data, which was used to develop the predictive tool, is given in Table 1 [11,12]. In six cases, the actual erosion yield is probably greater than the value listed because a portion or all of the exposed area of the flight sample was completely eroded away. In these cases, the measured erosion yields were also included in the data set to develop a predictive erosion yield equation because, in general, the samples appeared that they were completely eroded at a fluence level very close to the full mission fluence.

B. Modeling Variable Considerations

Upon a cursory inspection of the atomic oxygen erosion yields from the MISSE 2 PEACE polymers data, as well as previous LEO flight experiments, it was clear that polymers with a significant abundance of pendent fluorine and/or chlorine atoms (such as fluorinated ethylene propylene and chlorotrifluoroethylene) have low atomic oxygen erosion yields relative to Kapton H polyimide in LEO. Conversely, polymers with significant oxygen in their backbone (such as polyoxymethylene) had much higher atomic oxygen erosion yields. It is far less clear as to what degree the erosion yield depends upon mixes of in-the-chain or pendent oxygen, nitrogen, and benzyl rings and/or whether the bonding is single, double or triple. Thus, many approaches were explored to correlate chemical structure, the number atoms of each type in a polymer repeat unit, and number of bonds of each type (single, double, or triple as well as carbon bonding to what atoms) in the polymer repeat unit.

Polymer density was also considered as a potential erosion yield dependent variable because densely packed atoms should have lower erosion yields than loosely packed atoms because it would take more atoms to remove the same amount of volume. Data on polymer density was either obtained from supplier information or density gradient column testing.

Most polymers contain some fraction of inorganic material that does not become volatile upon reaction with atomic oxygen. The

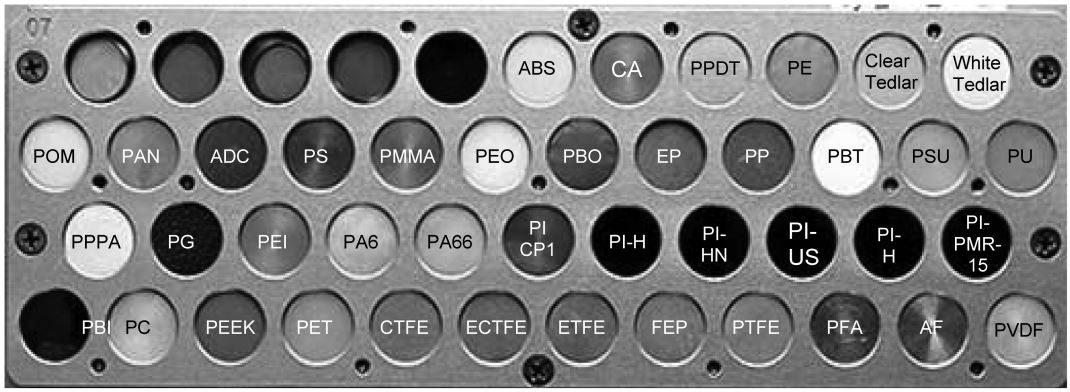

Fig. 2 Photograph of the MISSE 2 PEACE polymers experiment before flight. The labels shown indicate the materials defined in Table 1.

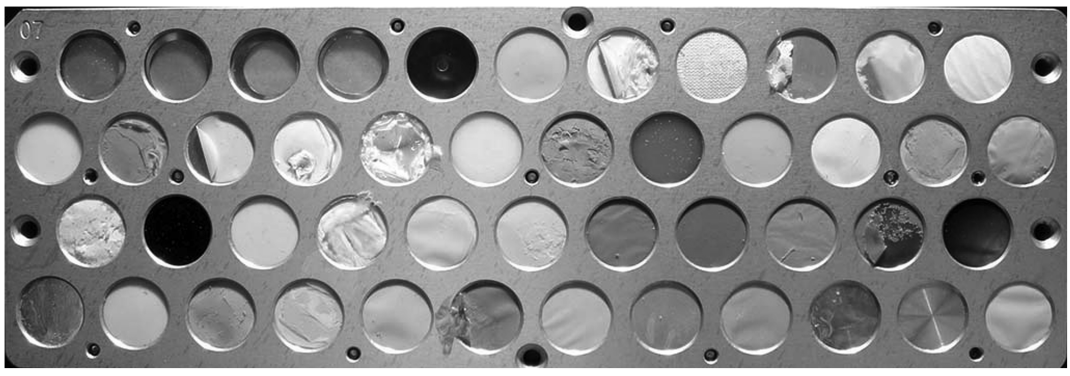

Fig. 3 Photograph of the MISSE 2 PEACE polymers experiment postflight.

Table 1 MISSE 2 PEACE polymers erosion yield data

Material	Polymer abbreviation	LEO MISSE 2 erosion yield, cm^3/atom
Acrylonitrile butadiene styrene	ABS	1.09E − 24
Cellulose acetate	CA	5.05E − 24
Poly-(*p*-phenylene terephthalamide)	PPDT (Kevlar)	6.28E − 25
Polyethylene	PE	>3.74E − 24
Polyvinyl fluoride	PVF (clear Tedlar)	3.19E − 24
Crystalline polyvinylfluoride with white pigment	PVF (white Tedlar)	1.01E − 25
Polyoxymethylene; acetal; polyformaldehyde	POM (Delrin)	9.14E − 24
Polyacrylonitrile	PAN	1.41E − 24
Allyl diglycol carbonate	ADC (CR-39)	>6.80E − 24
Polystyrene	PS	3.74E − 24
Polymethyl methacrylate	PMMA	>5.60E − 24
Polyethylene oxide	PEO	1.93E − 24
Poly(*p*-phenylene-2 6-benzobisoxazole)	PBO (Zylon)	1.36E − 24
Epoxide or epoxy	EP	4.21E − 24
Polypropylene	PP	2.68E − 24
Polybutylene terephthalate	PBT	9.11E − 25
Polysulphone	PSU	2.94E − 24
Polyurethane	PU	1.56E − 24
Polyphenylene isophthalate	PPPA (Nomex)	1.41E − 24
Pyrolytic graphite	PG	4.15E − 25
Polyetherimide	PEI	>3.31E − 24
Polyamide 6 or nylon 6	PA 6	3.51E − 24
Polyamide 66 or nylon 66	PA 66	1.80E − 24
Polyimide	PI (CP1)	1.91E − 24
Polyimide (PMDA)	PI (Kapton H)	3.00E − 24
Polyimide (PMDA)	PI (Kapton HN)	2.81E − 24
Polyimide (BPDA)	PI (Upilex-S or US)	9.22E − 25
High temperature polyimide resin	PI (PMR-15)	>3.02E − 24
Polybenzimidazole	PBI	>2.21E − 24
Polycarbonate	PC	4.29E − 24
Polyetheretherketone	PEEK	2.99E − 24
Polyethylene terephthalate	PET (Mylar)	3.01E − 24
Chlorotrifluoroethylene	CTFE (Kel-f)	8.31E − 25
Ethylene-chlorotrifluoroethylene	ECTFE (Halar)	1.79E − 24
Tetrafluorethylene-ethylene copolymer	ETFE (Tefzel)	9.61E − 25
Fluorinated ethylene propylene	FEP	2.00E − 25
Polytetrafluoroethylene	PTFE	1.42E − 25
Perfluoroalkoxy copolymer resin	PFA	1.73E − 25
Amorphous Fluoropolymer	AF	1.98E − 25
Polyvinylidene fluoride	PVDF (Kynar)	1.29E − 24

postatomic oxygen exposure residue is called ash. The presence of resulting fragile remaining ash may be a portion of the debris shown on or above some of the samples in the MISSE 2 PEACE polymers experiment postflight photo shown in Fig. 3. As atomic oxygen erodes a polymer that contains inorganic material in LEO, the resulting nonvolatile ash begins to accumulate on the eroded surface of the polymer, tending to shield the underlying polymer from oxidation. As a result, the ash content of polymers reduces the polymer's erosion yield by shielding the polymer from atomic oxygen. If one compares the erosion yield of clear polyvinyl fluoride (clear Tedlar) with that of white Tedlar, it becomes evident that the titanium dioxide pigment particles in white Tedlar shield its surface, resulting in a very low erosion yield of 0.101×10^{-24} cm^3/atom compared with a much higher erosion yield, 3.19×10^{-24} cm^3/atom, for clear Tedlar. Although the ash content expressed as a fractional volume of ash would be more correct when considering erosion yield effects, it is much easier to use the mass fraction of ash because the densities of the ash are difficult to measure.

Ash content used to develop the predictive tool described in this paper was determined experimentally for each of the 39 PEACE polymers (including Kapton H) and pyrolytic graphite. It was determined as the fraction of the initial dehydrated polymer mass that is nonvolatile and remains after the polymer has been completely oxidized in an RF plasma asher. This was accomplished by placing pieces of each polymer in thin aluminum foil cups that were previously exposed to atomic oxygen to remove organic coatings that typically reside on aluminum foil as a result of foil processing. The samples in the aluminum cups were then ashed for several hundred hours in a RF plasma asher operated on air until only ash remained. Figure 4 shows scanning electron microscope images of the ash remaining from white Tedlar and polyethylene oxide. Using energy dispersive spectroscopy the white Tedlar ash indicated the presence of titanium as expected for the titanium dioxide pigment particles and the ash from polyethylene oxide indicated a mix of metal elements.

Unfortunately, a gradual buildup of inorganic contamination from the asher itself complicates the process of determining ash content because the added mass from contaminants is observed as additional ash. This buildup is especially prevalent if the ashing is continued long after the organic portion of the polymer is completely oxidized. Additionally, materials with low erosion yields in the asher environment tend to accumulate more contamination than those with high erosion yields. The contamination is also difficult to correct for because it depends on the surface area of the ash which is difficult to measure.

The effect of ash content on erosion yield in an end Hall hyperthermal atomic oxygen facility [16] was determined by measuring the erosion yield of five epoxy resin samples which were purposely filled with various amounts of fumed silica. Epoxy resin with no-added fumed silica was found to also contain some ash as indicated in Table 2 as a result of ashing samples of the cured epoxy. An additional amount of ash, in the form of fumed silica, was weighed and mixed with both parts of the uncured epoxy to achieve a total mass fraction ash indicated in Table 2 which was used to plot Fig. 5.

The effect of the total mass fraction ash on the erosion yield was measured using an end Hall hyperthermal atomic oxygen source

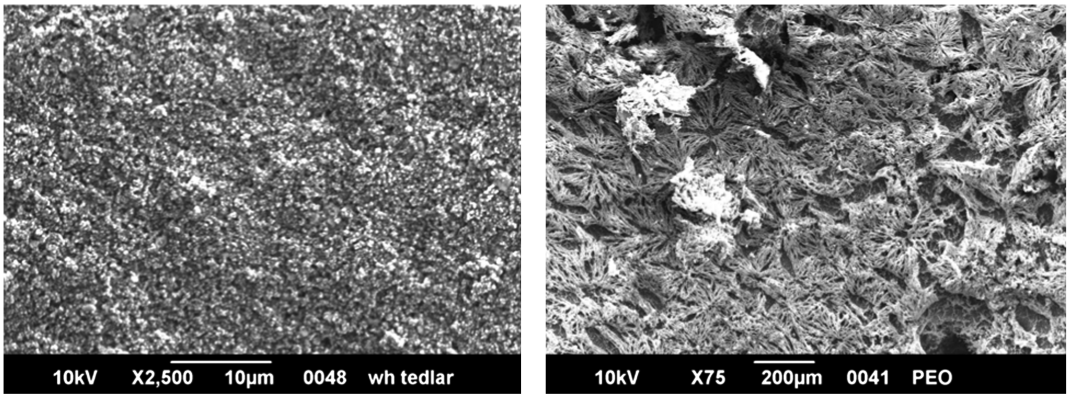

a) b)

Fig. 4 Scanning electron microscope images of the ash remaining after several hundred hours of RF plasma asher air plasma exposure: a) white Tedlar titanium dioxide ash particles and b) ash remaining from polyethylene oxide.

operated on pure oxygen at ~70 eV. It was necessary to use hyperthermal rather than thermal energy atomic oxygen attack because thermal energy atomic oxygen is not greatly attenuated (compared with LEO hyperthermal atomic oxygen) in reaction probability as a result of impingement upon ash surfaces. Because particle-filled epoxy resins tend to have a resin rich surface all the samples were abraded before atomic oxygen exposure to ensure that the surfaces exposed to atomic oxygen were representative of the bulk material.

The results of the erosion yield dependence upon mass fraction ash for a Kapton H effective fluence of 1.24×10^{20} atoms/cm^2 is shown in Fig. 5. The erosion yield of the neat epoxy resin (if there was no ash at all in the resin) was estimated based on the slope of the curve shown in Fig. 5 and the intercept at zero mass fraction ash.

The solid line in Fig. 5 is an equation which models the observed dependence given by

$$E_{ya} = E_{yo} e^{-KA/(1-A)} \tag{1}$$

Where the solid line represents the best fit between ash filled epoxy of Fig. 5 and ash filled Tedlar in Fig. 6. The erosion yield dependence function in Eq. (1) was designed to produce an erosion yield of zero if the ash mass fractional content is one and an erosion yield of E_{yo} if the ash content is zero (neat polymer). This observed erosion yield dependence on ash content was also quantifiably consistent with end Hall atomic oxygen exposure of clear and white Tedlar, thus suggesting that the equation is probably reasonably accurate for all ash-containing polymers.

The solid line in Fig. 6 represents the same Eq. (1) erosion yield dependency constant $K = 1.94$, as in the Fig. 5 plot.

Table 3 lists the density, ρ, and mass fraction of the polymer that is ash, A, measured for each of the MISSE 2 PEACE polymers. Use of a density gradient column and highly accurate density calibration samples allowed the density of many materials to be measured to five decimal places [11].

It is expected that the erosion yield attenuation constant, K, increases with fluence for ash-containing polymers as the surface of the ash-containing polymers becomes more covered with remaining ash with increasing atomic oxygen fluence. An approximation to this ash shielding dependence on fluence was made by modeling the erosion yield of white Tedlar in hyperthermal atomic oxygen environments for the low fluence end Hall test and the high-fluence MISSE 2 LEO exposure as shown in Fig. 7. In this figure the erosion yield for the end Hall test was corrected to account for the differences between the Kapton H effective fluence of the end Hall exposure and in-space exposure using the ratio between Kapton H and white Tedlar erosion yields for both environments.

A best fit curve drawn through the data is given by

$$K = (1.80 \times 10^{-16}) F^{0.76} \tag{2}$$

Although a linear fit could also be applied to the three data points in Fig. 7, the best fit is with a power law dependence which implies that if the fluence doubles the attenuation constant is slightly less than doubled. This is reasonable because the buildup of ash on the surface of a polymer, which causes the attenuation, occurs faster at low fluences when hyperthermal atomic oxygen is impacting the polymer. As a greater fluence is experienced, the ash builds up on the surface of the polymer which tends to begin to shield the underlying polymer from attack.

Additional erosion yield dependencies were considered for the predictive model including the physical density, ρ (in grams/cm^3). For example, a foam polymer would have a high erosion yield compared with a fully dense polymer. Also considered was the packing density of atoms, V_Σ/V_r, which relates to how densely the atoms theoretically could be packed in comparison to the actual volume of the repeat unit where larger spaces would occur between atoms due to van der Waals bonding or void spaces. Loosely packed atoms should result in a high erosion yield compared with densely packed atoms. The minimum volume of the atoms that make up a polymer repeat unit, V_Σ, was based on the sum of the atoms making up the polymer repeat unit assuming each atom's volume is determined by its covalent radii.

The actual volume, V_r, of each repeat unit was determined based on the chemical structure of the repeat unit as well as the molecular weight and density of the material. Thus, if the ratio of V_Σ/V_r was much less than one, the polymer's erosion yield would be higher than that of a similarly structured polymer with tightly packed atoms. Values of V_Σ/V_r are given in [15].

Table 2 Ash content of the five samples used to measure erosion yield dependence on mass fraction ash

Mass fraction of ash in as-received epoxy	Mass fraction of fumed silica added (as ash) to epoxy	Total mass fraction ash of sample	Ratio of atomic oxygen erosion yield relative to neat (no ash) polymer
0.0453	0.0000	0.0453	0.912
0.0453	0.0837	0.1252	0.758
0.0453	0.1662	0.2039	0.758
0.0453	0.3336	0.3638	0.330
0.0453	0.4167	0.4431	0.214
0.0453	0.4998	0.5225	0.120

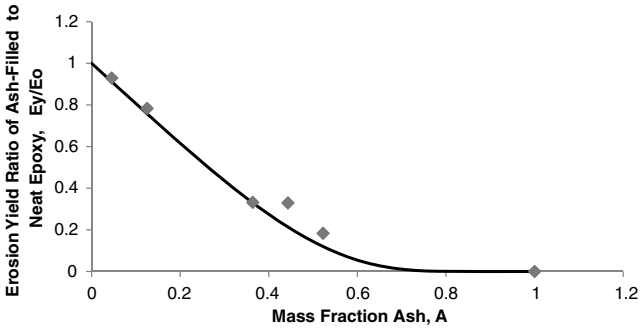

Fig. 5 Erosion yield dependence on mass fraction ash in epoxy for a Kapton H effective fluence of 1.24×10^{20} atoms/cm^2.

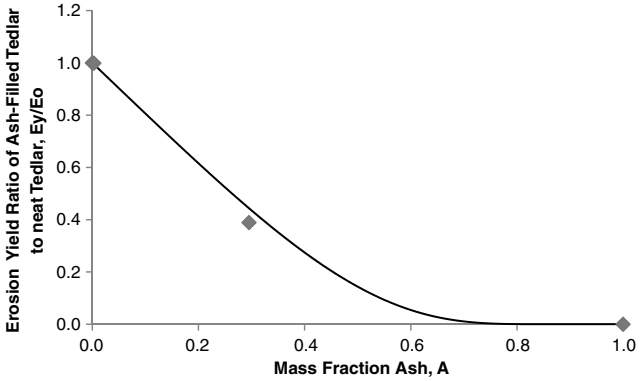

Fig. 6 Erosion yield of Tedlar relative to neat Tedlar as a function of ash.

III. Results and Discussion

A. Single Organic Material Erosion Yield Prediction

Over 100 different types of equations were tested using the information in the previous section to determine a formula with a high correlation coefficient, R^2, with the actual LEO erosion yield data. An initial erosion yield model (published in December 2009) produced a correlation coefficient of 0.914. That model used a linear assumption of dependency relations and made extensive use of bonding information of the atoms in a repeat unit [16]. However, the equation for that model was found to produce negative erosion yields in some cases for polymers that were not flown as part of the MISSE 2 PEACE polymers experiment.

To correct this problem, an alternative approach (September 2009 version) was then pursued, which used the dependency variables (such as atomic populations per repeat unit) as exponents with appropriate constants to optimize the correlation coefficient. This concept used weighted exponents rather than weighted additive terms allows dependency upon the variables of number and types of chemical bonds, polymer density information, and fractional ash content data and atomic oxygen fluence prevented negative erosion yield values and enabled significant simplification of the predictive equation with very little loss in the correlation coefficient from the September 2009 version.

Table 3 MISSE 2 PEACE polymers density and fractional ash content

Material	Polymer abbreviation	Density [12], ρ, g/cm^3	Mass fraction of polymer that is ash [15], A
Acrylonitrile butadiene styrene	ABS	1.05	0.0458
Cellulose acetate	CA	1.2911	0.00283
Poly-(p-phenylene terephthalamide)	PPDT (Kevlar)	1.4422	0.00372
Polyethylene	PE	0.918	0.0203
Polyvinyl fluoride	PVF (clear Tedlar)	1.3792	0.00285
Crystalline polyvinylfluoride with white pigment	PVF (white Tedlar)	1.6241	0.295
Polyoxymethylene; acetal; polyformaldehyde	POM (Delrin)	1.3984	0.00902
Polyacrylonitrile	PAN	1.1435	0.00184
Allyl diglycol carbonate	ADC (CR-39)	1.3173	0.00265
Polystyrene	PS	1.0503	0.00042
Polymethyl methacrylate	PMMA	1.1628	0.00028
Polyethylene oxide	PEO	1.1470	0.00112
Poly(p-phenylene-2 6-benzobisoxazole)	PBO (Zylon)	1.3976	0.0109
Epoxide or epoxy	EP	1.1150	0.0304
Polypropylene	PP	0.9065	0.00184
Polybutylene terephthalate	PBT	1.3318	0.0629
Polysulphone	PSU	1.2199	0.00348
Polyurethane	PU	1.2345	0.00664
Polyphenylene isophthalate	PPPA (Nomex)	0.72	0.0476
Pyrolytic graphite	PG	2.22	0.00154
Polyetherimide	PEI	1.2873	0.00105
Polyamide 6 or nylon 6	PA 6	1.1233	0.00388
Polyamide 66 or nylon 66	PA 66	1.2252	0.00459
Polyimide	PI (CP1)	1.4193	0.00171
Polyimide (PMDA)	PI (Katpon H)	1.4273	0.00284
Polyimide (PMDA)	PI (Kapton HN)	1.4345	0.00441
Polyimide (BPDA)	PI (Upilex-S or US)	1.3866	0.00164
High temperature polyimide resin	PI (PMR-15)	1.3232	0.000531
Polybenzimidazole	PBI	1.2758	0.000927
Polycarbonate	PC	1.1231	0.000992
Polyetheretherketone	PEEK	1.2259	0.00177
Polyethylene terephthalate	PET (Mylar)	1.3925	0.00826
Chlorotrifluoroethylene	CTFE (Kel-f)	2.1327	0.00204
Ethylene-chlorotrifluoroethylene	ECTFE (Halar)	1.6761	0.000655
Tetrafluorethylene-ethylene copolymer	ETFE (Tefzel)	1.7397	0.00123
Fluorinated ethylene propylene	FEP	2.1443	0.00534
Polytetrafluoroethylene	PTFE	2.1503	0.0427
Perfluoroalkoxy copolymer resin	PFA	2.1383	0.000298
Amorphous fluoropolymer	AF	2.1463	0.0362
Polyvinylidene fluoride	PVDF (Kynar)	1.7623	0.0358

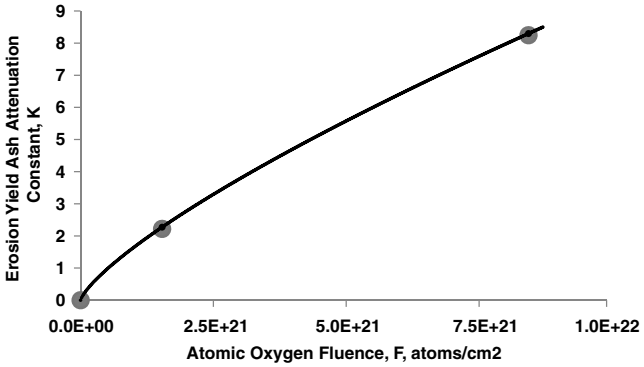

Fig. 7 Erosion yield ash attenuation constant, *K*, as a function of fluence, *F*.

This simpler approach resulted in a reasonably high correlation coefficient with actual LEO MISSE 2 PEACE polymer data. The resulting equation used atomic populations in the repeat unit as well as physical density, packing density, ash content, and the number of single and double oxygen bonds in the repeat unit. The predictive LEO erosion yield equation is given by

$$E_y = C_o(V_\Sigma/V_r)^{C_{\Sigma/r}}(\rho)^{C\rho}e^X \tag{3}$$

where

$$\begin{aligned} X = {} & (C_{C/t}N_C + C_{H/t}N_H + C_{sO/t}N_{sO} + C_{dO/t}N_{dO} \\ & + C_{N/t}N_N + C_{Cl/t}N_{Cl} + C_{F/t}N_F + C_{S/t}N_S)/N_t) \\ & + (C_{O/C}N_O + C_{N/C}N_N + C_{F/C}N_F + C_{H/C}N_H \\ & + C_{Cl/C}N_{Cl} + C_{S/C}N_S)/N_C - K[(A)]/(1-A) \end{aligned} \tag{4}$$

and

$$K = (1.80 \times 10^{-16})F^{0.76} \tag{5}$$

The C coefficients C_o, $C_{\Sigma/r}$, C_ρ, $C_{C/t}$, $C_{H/t}$, $C_{sO/t}$, $C_{dO/t}$, $C_{N/t}$, $C_{Cl/t}$, $C_{F/t}$, $C_{S/t}$, $C_{O/C}$, $C_{N/C}$, $C_{F/C}$, $C_{H/C}$, $C_{Cl/C}$, $C_{S/C}$, and K are constants associated with the various terms relating to the number of atoms, bonds, or physical characteristics of the polymers. The first set of terms $(V_\Sigma/V_r)^{C_{\Sigma/r}}$ relates to how densely the atoms are packed compared with how dense they could theoretically be packed. Loosely packed polymer atoms should have a higher erosion yield than densely packed atoms. Thus, the $(V_\Sigma/V_r)^{C_{\Sigma/r}}$ term is the ratio of volume computed by from the covalent radii atoms to the actual volume based on the molecular weight and density. The constant $C_{\Sigma/r}$ is the exponential weighting factor which prevents negative values of the erosion yield yet allows dependency upon the packing ratio. The $(\rho)^{C\rho}$ term, in a similar manner, addresses the variations in density of materials with an exponential constant, $C\rho$. The term e^x addresses the number and types of chemical bonds relative to the total number of atoms or carbon atoms in the polymer repeat unit where X is exponential weighted sum of all the numbers and types of bonds in the polymer repeat unit. The $-K[(A)]/(1-A)$ term in Eq. (4) for the exponent X models the ash content effect on the erosion yield in a manner as previously described by Eq. (1) where the constant, K, is fluence dependent as described by Eq. (2).

All of the C coefficients for the Eq. (3) were optimized to produce the highest correlation coefficient possible using the available data. This produced a correlation coefficient between predicted erosion yield and LEO measured erosion yield is 0.895. This correlation includes all of the MISSE 2 PEACE polymers except polyethylene oxide, which appeared to have an anomalously low erosion yield, for some unknown reason, compared with what is predicted based on the chemical and physical properties. The values of the optimized C coefficients are listed in Table 4.

A plot of the optimized predicted erosion yields versus the LEO measured MISSE 2 PEACE polymer experiment erosion yields [with the exception of polyethylene oxide (PEO)] using Eq. (4) and the constants in Table 4 is shown in Fig. 8.

The resulting predicted erosion yields have a correlation coefficient of 0.895 and an uncertainty (standard deviation) of $\pm 1.27 \times 10^{-24}$ cm^3/atom when comparing predicted erosion yields with actual space erosion yields (for 38 polymers and pyrolytic graphite). The predictive tool of Eqs. (3) and (4) allows for erosion yield prediction at any atomic oxygen fluence. This is especially relevant for polymers containing high fractional ash contents. A table listing the materials, their predicted erosion yields for the MISSE 2 fluence, and MISSE 2 measured erosion yields is given in Table 5.

These results represent a significant improvement over the earliest atomic oxygen erosion yield predictive tool [13] as a result of having additional physical and chemical properties of the materials tested, having actual and accurate in-space erosion yield data, taking into account polymer ash content, possibly using a different modeling formula.

B. Mixed Organic Materials and Carbon Fiber Polymer Matrix Composites

Carbon fiber-filled organic matrix composites contain materials of two different erosion yields. Foam (open or closed pore) materials also have a higher erosion yield than their fully dense versions. If one simply uses the rule of mixtures based on the erosion yields of each

Table 4 Definition and values of the optimized coefficients associated with each variable

Symbol	Definition	Value
C_O	Proportionality constant which resulted from best fit linear equation relating the measured atomic erosion yield to predicted erosion yield	3.02×10^{30} cm^3/atom
$C_{sO/t}$	Constant for single bonded oxygen atoms in the polymer repeat unit	−0.94
$C_{dO/t}$	Constant for double bonded oxygen atoms in the polymer repeat unit	−3.59
$C_{N/t}$	Constant for nitrogen atoms in the polymer repeat unit	4.42
$C_{S/t}$	Constant for sulfur atoms in polymer repeat unit	−22.0
$C_{Cl/t}$	Constant for chlorine atoms in polymer repeat unit	−8.60
$C_{F/t}$	Constant for fluorine atoms in polymer repeat unit	−1.54
$C_{\Sigma/r}$	Constant for ratio of sum of volume of atoms in repeat unit (based on their covalent radii) to volume of the repeat unit	−2.86
$C_{S/C}$	Constant for the ratio of sulfur atoms to carbon atoms in the repeat unit	3.90
C_ρ	Constant for polymer density	4.87
$C_{O/C}$	Constant for the ratio of oxygen atoms to carbon atoms in the repeat unit	0.395
$C_{F/C}$	Constant for the ratio of the fluorine atoms to carbon atoms in the repeat unit	−1.70
$C_{H/C}$	Constant for the ratio of the hydrogen atoms to carbon atoms in the repeat unit	0.053
$C_{N/C}$	Constant for the ratio of the nitrogen atoms to carbon atoms in the repeat unit	−5.02
$C_{Cl/C}$	Constant for the ratio of the chlorine atoms to carbon atoms in the repeat unit	1.48
K	Erosion yield ash attenuation constant	8.30 for a fluence of 8.43×10^{21} atoms/cm^2

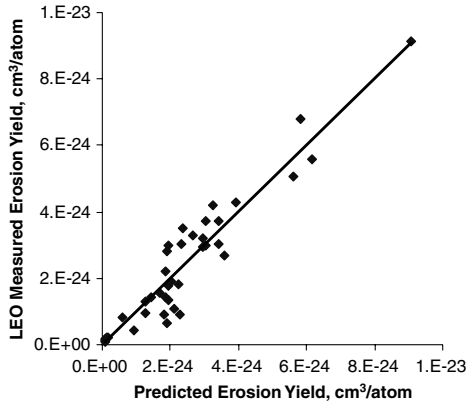

Fig. 8 Optimized linear fit between the LEO MISSE 2 PEACE atomic oxygen erosion yields and the predicted erosion yields for the MISSE 2 mission with an atomic oxygen fluence of 8.43×10^{21} atoms/cm^2.

material and the volume fraction of each material then an incorrect erosion yield of the mixture is predicted. This fact can be illustrated by considering a foamed polymer that is one half polymer and one half pores. The erosion yield of the polymer half would simply be the erosion yield of the normal fully dense polymer. However, the erosion yield of pores is infinity because it does not take any oxygen atoms to erode through a pore. Thus, using the rule of mixtures based on the erosion yields of each material one would predict an infinite erosion yield of the mixed material.

However if you use the rule of mixtures based on the erosion resistance of each material and the volume fraction of each material then a correct erosion yield is predicted for the mixture. The erosion resistance is simply the inverse of the erosion yield. The concept is similar to adding electrical resistors in parallel to obtain the overall resistance. Thus, the erosion resistance, E_R, of the mixed materials is given by

$$E_R = \frac{1}{E_y} = F_f E_{Rf} + F_P E_{Rp} \tag{6}$$

The atomic oxygen erosion yield of the fiber-filled composite, written in terms of erosion yields, is thus given by

$$E_y = 1/(F_f/E_{yf} + F_P/E_{yp}) \tag{7}$$

Although data is not yet available to validate this technique for determining erosion yields of mixed materials, the process appears to make logical sense and give reasonable and expected values provided that both the fibers and the polymer have nonzero erosion yields. The ash content of a carbon fiber based hydrocarbon matrix composite can be evaluated by ashing samples (typically using filings) of composite. This would allow the matrix polymer and fiber components of the composite to contribute in proper proportions to the ash content. If the polymer matrix material is a copolymer which contains polysiloxanes then using the erosion yield for that polymer which includes its ash content should be used in the preceding formula.

Table 5 Comparison of predicted and measured atomic oxygen erosion yields

Material	Polymer abbreviation	Predicted erosion yield, cm^3/atom	MISSE 2 erosion yield, cm^3/atom
Acrylonitrile butadiene styrene	ABS	2.12E − 24	1.09E − 24
Cellulose acetate	CA	5.63E − 24	5.05E − 24
Poly-(*p*-phenylene terephthalamide)	PPD-T (Kevlar)	1.92E − 24	6.28E − 25
Polyethylene	PE	3.04E − 24	>3.74E − 24
Polyvinylfluoride - clear	PVF (clear Tedlar)	2.94E − 24	3.19E − 24
Polyvinyl fluoride - with white pigment	PVF (white Tedlar)	9.39E − 26	1.01E − 25
Polyoxymethylene; acetal; polyformaldehyde	POM (Delrin)	9.03E − 24	9.14E − 24
Polyacrylonitrile	PAN	1.42E − 24	1.41E − 24
Allyl diglycol corbonate	ADC (CR-39)	5.83E − 24	>6.80E − 24
Polystyrene	PS	3.43E − 24	3.74E − 24
Polymethyl methacrylate	PMMA	6.17E − 24	>5.60E − 24
Polyethylene oxide	PEO	7.02E − 24	1.93E − 24
Poly-(*p*-phenylene-2 6-benzobisoxazole)	PBO (Zylon)	1.91E − 24	1.36E − 24
Epoxide or Epoxy	EP	3.24E − 24	4.21E − 24
Polypropylene	PP	3.58E − 24	2.68E − 24
Polybutylene terephthalate	PBT	2.31E − 24	9.11E − 25
Pulysulphone	PSU	2.95E − 24	2.94E − 24
Polyurethane	PU	1.73E − 24	1.56E − 24
Polyphenylene isophthalate	PPPA (Nomex)	1.84E − 24	1.41E − 24
Pyrolytic graphite	PG	9.41E − 25	4.15E − 25
Polyetherimide	PEI	2.66E − 24	>3.31E − 24
Polyamide 6 or nylon 6	PA 6	2.40E − 24	3.51E − 24
Polyamide 66 or nylon 66	PA 66	2.28E − 24	1.80E − 24
Polyimide	PI (CP1)	2.02E − 24	1.91E − 24
Polyimide (PMDA)	PI (Kapton HN)	1.91E − 24	2.81E − 24
Polyimide (BPDA)	PI (Upilex-S)	1.83E − 24	9.22E − 25
Polyimide (PMDA)	PI (Kapton H)	1.93E − 24	3.00E − 24
High temperature polyimide resin	PI (PMR-15)	2.33E − 24	>3.02E − 24
Polybenzimidazole	PBI	1.83E − 24	>2.21E − 24
Polycarbonate	PC	3.94E − 24	4.29E − 24
Polyetheretherketone	PEEK	3.03E − 24	2.99E − 24
Polyethylene terephthalate	PET (Mylar)	3.44E − 24	3.01E − 24
Chlorotrifluoroethylene	CTFE (Kel-f)	6.03E − 25	8.31E − 25
Ethylene-chlorotrifluoroethylene	ECTFE (Halar)	1.94E − 24	1.79E − 24
Tetrafluoroethylene-ethylene copolymer	ETFE (Tefzel)	1.26E − 24	9.61E − 25
Fluorinated ethylene propylene	FEP	9.82E − 26	2.00E − 25
Polytetrafluoroethylene	PTFE	7.09E − 26	1.42E − 25
Polyvinylidene fluoride	PVDF (Kynar)	1.26E − 24	1.29E − 24
Perfluoroalkoxy copolymer resin	PFA	7.54E − 26	1.73E − 25
Amorphous fluoropolymer	AF	1.38E − 25	1.98E − 25

IV. Conclusions

A predictive tool was developed to estimate the LEO atomic oxygen erosion yield of polymers based on the results of the MISSE 2 PEACE polymers experiment, which accurately measured the erosion yield of a wide variety of polymers and pyrolytic graphite. The flight experiment materials were selected specifically to represent a variety of polymers used in space as well as a wide variety of polymer chemical structures. The September 2009 version predictive tool uses the chemical structure, atomic populations of the polymer repeat unit, oxygen bonding information, and physical properties (such as density and ash content) that can be measured in ground laboratory tests. The prediction does not require the use of asher erosion yield information. The tool has a correlation coefficient of 0.895 and an uncertainty of $\pm 1.27 \times 10^{-24}$ cm^3/atom when compared with actual MISSE 2 PEACE polymers space data (for 38 polymers and pyrolytic graphite). One polymer, PEO, was found to be significantly off the linear fit for some unknown reason and was not used in the predictive tool equation. The predictive tool does appear to predict reasonable atomic oxygen erosion yields, even for those polymers that yielded a negative erosion value with the previous predictive process. The tool also allows for the prediction of atomic oxygen erosion yields as a function of fluence which is relevant for polymers containing high ash contents. A technique for predicting the atomic oxygen erosion yield of composite materials was identified based on the rule of mixtures and an electrical analogue to erosion yield. The intent of the predictive tool is to be able to make estimates of LEO atomic oxygen erosion yields for new polymers and composites without requiring expensive and time consumptive in-space testing.

References

[1] Leger, L. J., Spiker, I. K., Kuminecz, J. F., Ballentine, T. J., and Visentine, J. T., "STS Flight 5 LEO Effects Experiment: Background and Description of Thin Film Results," AIAA Paper 83-2631-CP, Oct. 1983.

[2] Smith, K. A., "Evaluation of Oxygen Interaction with Materials (EOIM): STS-8, Atomic Oxygen Effects," AIAA Paper 85-7021, Nov. 1985.

[3] Banks, B. A., Mirtich, M. J., Rutledge, S. K., and Swec, D. M., "Sputtered Coatings for Protection of Spacecraft Polymers," 11th International Conference on Metallurgical Coatings, San Diego, CA, 9–13 April 1984.

[4] Banks, B. A., and Rutledge, S. K., "Low Earth Orbital Atomic Oxygen Simulation for Materials Durability Evaluation," Proceedings of the Fourth European Symposium on Spacecraft Materials in Space Environment, Toulouse, France, 6–9 Sept. 1988.

[5] Banks, B. A., "The Use of Fluoropolymers in Space Applications," *Modern Fluoropolymers*, edited by John Scheirs, Wiley, New York, 1997, Chap. 4, pp. 103–113.

[6] ASTM E 2089-00, "Standard Practices for Ground Laboratory Atomic Oxygen Interaction Evaluation of Materials for Space Applications," June 2000.

[7] Slemp, W. S., Santos-Mason, B., Bykes, G. F., Jr., and Witte, W. S., Jr., "Effects of STS-8 Atomic Oxygen Exposure on Composites, Polymeric Films and Coatings," AIAA Paper 85-0421, Jan. 1985.

[8] Smith, K., "Evaluation of Oxygen Interaction with Materials (EOIM): STS-8," AIAA Paper 85-7021, AIAA Shuttle Environment and Operations 2 Conference, Houston, TX, Nov. 1985.

[9] Silverman, E., "Space Environmental Effects on Spacecraft LEO Materials Selection Guide," NASA CR 4661, Aug. 1995.

[10] de Groh, K. K., Banks, B. A., McCarthy, C. E., Rucker, R. N., Roberts, L. M., and Berger, L. A., "MISSE 2 PEACE Polymers Atomic Oxygen Erosion Experiment on the International Space Station," *High Performance Polymers*, Vol. 20, Nos. 4–5, Aug.–Oct. 2008, pp. 388–409.
doi:10.1177/0954008308089705

[11] de Groh, K. K., Banks, B. A., McCarthy C. E., Rucker, R. N., Roberts, L. M., and Berger, L. A., "MISSE PEACE Polymers Atomic Oxygen Erosion Results," NASA TM 2006-214482, Nov. 2006.

[12] Integrity Testing Lab., "Prediction of Erosion of Polymer-Based Materials by Atomic Oxygen in LEO," NASA CR C-72917-G, 1998.

[13] Kleiman, J., Iskanderova, Z., Banks, B. A., de Groh, K. K., and Sechkar, E., "Prediction and Measurement of the Atomic Oxygen Erosion Yield of Polymers in Low Earth Orbital Flight," Eigth International Symposium on Materials in a Space Environment and the Fifth International Conference on Protection of Materials and Structures from the LEO Space Environment, Arcachon, France, 4–9 June 2000.

[14] Minton, D. J., Stockdale, D. P., Lee, D., Yu, L., and Minton, T., "Probing the Effects of Molecular Structure on the Erosion of Hydrocarbon-Based Polymers by Atomic Oxygen," 10th International Symposium on Materials in a Space Environment and Eighth International Conference on Protection of Materials and Structures in a Space Environment, Collioure, France, 19–23 June 2006.

[15] Banks, B. A., Backus, J. A., and de Groh, K. K., "Atomic Oxygen Erosion Yield Predictive Tool for Spacecraft Polymers in Low Earth Orbit," NASA TM-2008-215490, Dec. 2008.

[16] Banks, B. A., Waters, D. L., Thorson, S. D., de Groh, K. K., Snyder, A., and Miller, S. K., "Comparison of Atomic Oxygen Erosion Yields of Materials at Various Energies and Impact Angles," 10th International Symposium on Materials in a Space Environment and the Eighth International Conference on the Protection of Materials, NASA TM-2006-214363, Aug. 2006, Collioure, France, 19–23 June 2006.

D. Edwards
Associate Editor